

Phase equilibria and crystallochemical properties of Mg-chlorite

DAVID M. JENKINS*

Department of the Geophysical Sciences, University of Chicago, Chicago, Illinois 60637

JOSEPH V. CHERNOSKY, JR.

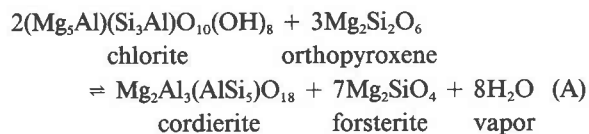
Department of the Geological Sciences, University of Maine at Orono, Orono, Maine 04473

ABSTRACT

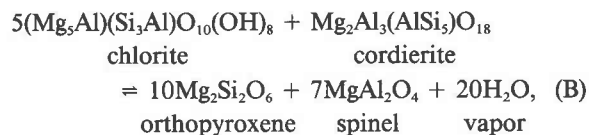
New experimental data on the upper thermal stability of chlorite in the system H_2O - MgO - Al_2O_3 - SiO_2 are reported here and are combined with other experimental data, molar volumes of the solid phases, heat capacities, H_2O fugacities, and activity expressions for cordierite, chlorite, and orthopyroxene to obtain an array of univariant curves about an invariant point at $720 \pm 10^\circ C$ and 2.75 ± 0.3 kbar where chlorite, cordierite, forsterite, orthopyroxene, spinel, and water are in equilibrium. A crystallochemical study of chlorite synthesized from three different bulk compositions at 3 and 14 kbar and over the temperature range of 650 – $850^\circ C$ suggests that Mg-chlorite attains a composition of $(Mg_{4.8}Al_{1.2})(Si_{2.8}Al_{1.2})O_{10}(OH)_8$ at its upper thermal stability at all pressures. Thermochemical data for clinocllore were derived from the experimental data on the dehydration of chlorite above 3.5 kbar, yielding values of -8220.452 ± 27 kJ/mol and -2186.2 ± 33 J/(K·mol) for ΔG_f° and ΔS_f° , respectively, at 1 bar and 298 K.

INTRODUCTION

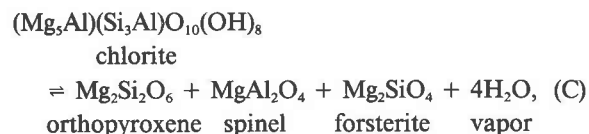
Chlorite is observed as a common rock-forming mineral within pelitic, mafic, ultramafic, and calc-silicate assemblages. To a close approximation, natural trioctahedral chlorite compositions can be expressed as binary combinations of the endmembers $(Fe_3^+Al)(Si_3Al)O_{10}(OH)_8$ (daphnite) and $(Mg_5Al)(Si_3Al)O_{10}(OH)_8$ (clinocllore) (e.g., Shirozu, 1978). The upper thermal stability of Mg-rich chlorite in ultramafic and calc-silicate assemblages involves the phases cordierite, spinel, forsterite, orthopyroxene, and water in the array of univariant curves that is shown schematically in Figure 1. Although there is a considerable amount of experimental data concerning chlorite phase relations in the simplified system H_2O - MgO - Al_2O_3 - SiO_2 (e.g., Fawcett and Yoder, 1966; Chernosky, 1974; Staudigel and Schreyer, 1977), there has been relatively little work on chlorite-cordierite relations below 3 kbar and no rigorous reversals of Reaction C (Fig. 1) between 3 and 10 kbar (Zen, 1972). There is also considerable disagreement within the literature (e.g., Shirozu and Momoi, 1972) concerning the unit-cell parameters of clinocllore and the degree to which they change with composition (primarily as a result of the exchange of Mg and Si for Al). The purposes of this study are to (1) establish a well-calibrated graph of the shift in the c parameter of Mg-chlorite as a function of the Al_2O_3 content, (2) present new experimental data for the reactions (written in terms of the endmember phases)



and



(3) compile new and existing experimental data for the reaction



and (4) derive thermodynamic data for clinocllore that agree with the extant experimental data.

Table 1 lists abbreviations and symbols used throughout this article.

EXPERIMENTAL TECHNIQUES

The experimental results discussed in the following sections were obtained at the University of Maine and at the University of Chicago using different starting materials and experimental techniques. At present, we believe that the differences between starting materials and experimental techniques are insignificant and that the results from both laboratories are directly comparable. Nevertheless, even small differences in experimental techniques may become significant in view of future investigations,

* Present address: Department of Geological Sciences, State University of New York-Binghamton, Binghamton, New York 13901.

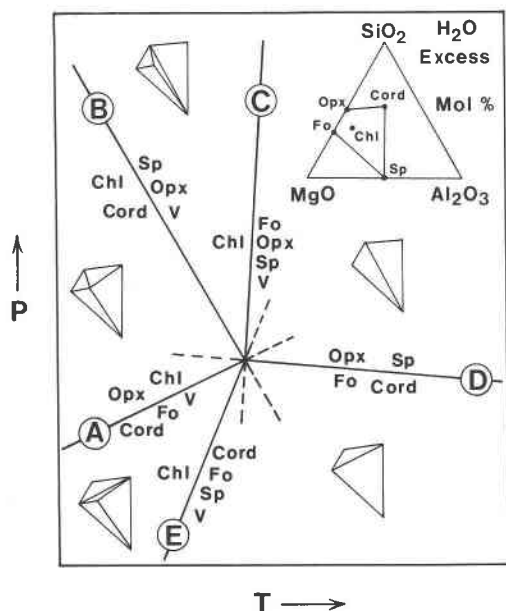


Fig. 1. Schreinemaker's analysis of univariant curves about the invariant point involving chlorite (Chl), cordierite (Cord), forsterite (Fo), orthopyroxene (Opx), spinel (Sp), and excess H₂O (V) in the system H₂O-MgO-Al₂O₃-SiO₂. Letters refer to reactions in the text.

and, therefore, the techniques used and results obtained in each laboratory are clearly distinguished.

Apparatus

Three types of experimental apparatus were used depending on the pressure range of the experiments. Experiments in the range 0.5–6 kbar were performed in cold-seal vessels at the University of Maine according to the procedure described by Chernosky (1982); pressures were measured with factory-calibrated Heise gauges and temperatures were measured with calibrated, sheathed, chromel-alumel thermocouples. Pressure measurements are believed accurate to ± 50 bars of the stated value, and temperature uncertainties are reported as ± 2 standard deviations about the mean temperature for each experiment. Experiments in the range 6–8 kbar were made in an internally heated gas vessel at the University of Chicago according to the procedure described by Jenkins (1983); pressures were measured with a factory-calibrated manganin cell (with an estimated accuracy of ± 50 bars), and the temperature gradients (3–8°) across the charges were measured with two calibrated, sheathed, chromel-alumel thermocouples. Experiments in the range of 10–14 kbar were performed in a piston-cylinder apparatus at the University of Chicago using a $\frac{3}{4}$ -in. NaCl assemblage. Using the procedure described by Jenkins (1981), sample pressures are within 300 bars of the gauge pressure, and temperatures, measured with chromel-alumel thermocouples, are believed to be accurate to $\pm 5^\circ\text{C}$.

Starting materials

All phases were synthesized from mixtures of oxides and/or hydroxides. Reagents used at the University of Maine were MgO (Fisher, lot 787699), fused SiO₂ (Corning lump cullet 7940, lot 62221), and γ -Al₂O₃, prepared by firing AlCl₃·6H₂O (Fisher, lot 792733) at 400°C for 2 h, at 700°C for 5 h, and at 900°C for 1 h. Reagents used at the University of Chicago were MgO, either

Table 1. Abbreviations and symbols

Chl	Chlorite	(Mg,Al) ₆ (Si,Al) ₄ O ₁₀ (OH) ₈
Cord	Cordierite	Mg ₂ Al ₃ (AlSi ₅)O ₁₈ ·nH ₂ O
Fo	Forsterite	Mg ₂ SiO ₄
Opx	Orthopyroxene	(Mg,Al) ₂ (Si,Al) ₂ O ₆
Sp	Spinel	MgAl ₂ O ₄
°	Superscript indicating the property of a pure phase at 1 bar and a given temperature.	
A	Activity of component i in phase A.	
a _i	Standard state is unit activity for the pure phase at the pressure and temperature of interest.	
C _p	Heat capacity at constant pressure (1 bar).	
f _{H₂O}	Fugacity of pure H ₂ O at a given pressure (P) and temperature (T) referenced to the ideal gas at 1 bar and T.	
ΔG _f [°] , ΔH _f [°] , ΔS _f [°]	Free energy, enthalpy, and entropy, respectively, of formation of a pure phase from the elements in their reference states at 298K and 1 bar.	
ΔG [°] , ΔS [°]	Free energy and entropy change, respectively, of reaction at 298K and 1 bar.	
G'	A symbol representing the summation of the right-hand terms of equation 3.	
S _T [°]	Third-law entropy of a pure phase at temperature T.	
v _{P,T} ^{solid}	Volume of one mole of a pure solid phase at the designated pressure and temperature.	
X _i ^A	Mole fraction of component i in phase A.	
X	Cations of Al in the chlorite formula (Mg _{6-X} Al _X)(Si _{4-X} Al _X)O ₁₀ (OH) ₈ .	

from single crystals (Mussel Shoals Electrochemical Co.) or fired from hydrous MgCO₃ (Baker, lot 36416); fused SiO₂; and Al₂O₃, either as α -Al₂O₃ (Baker Ultrex, lot 4901) or as Al(OH)₃ (Malinckrodt, checked gravimetrically for stoichiometry).

The compositions and synthesis conditions of the phases used to investigate Reactions A, B, and C are recorded in Table 2. All phases used at the University of Maine were synthesized hydrothermally, whereas only clinocllore was synthesized hydrothermally at the University of Chicago. Each synthetic phase was carefully inspected for purity using both optical and X-ray diffraction techniques. Synthetic clinocllore ($X = 1.0$) consisted of aggregates of fine-grained (5–30 μm) plates having an X-ray diffraction pattern corresponding to the 11b-layer polytype (Bailey and Brown, 1962; Carroll, 1970). An extensive discussion of the lattice parameters of clinocllore is given below. Hydrothermally synthesized cordierite, though free of impurities, was found to have numerous inclusions of what appeared to be entrapped water. After a 5-d heat treatment at 900°C to drive off entrapped water and to anneal the structure, the unit-cell parameters were found to be $a = 17.086(1)$ (uncertainty in last digit), $b = 9.740(8)$, and $c = 9.353(4)$ Å. Enstatite, with the unit-cell parameters $a = 18.222(3)$, $b = 8.822(1)$, and $c = 5.174(1)$ Å, was used for Reactions A and B. An aluminous enstatite with about 4 wt% Al₂O₃ was used for investigating Reaction C because this is the approximate composition of orthopyroxene in equilibrium with forsterite and spinel (Gasparik and Newton, 1984). The spinel and forsterite used in both laboratories were virtually identical, with $a = 8.079(3)$ and $8.083(1)$ Å for the spinel synthesized at Maine and Chicago, respectively, and d_{130} values (Schwab and Küstner, 1977) of 2.764 and 2.765 Å for the forsterite synthesized at Maine and Chicago, respectively. It is believed that spinel does not deviate significantly from the composition MgAl₂O₄ (i.e., show solubility toward Al₂O₃) throughout these reactions because of its coexistence with the Mg-rich phases forsterite and cordierite (Schreyer and Schairer, 1961) and because no significant shift in the X-ray peak positions was observed.

Table 2. Compositions and synthesis conditions of phases used for investigating Reactions A, B, and C

Phase (code number)	Composition	Synthesis conditions			Lab*	Starting mixtures Reaction		
		T (°C)	P	t (hours)		A	B	C
Clinocllore	(Mg ₅ Al)(Si ₃ Al)O ₁₀ (OH) ₈	650	3 kbar	500-1200	M	X	X	0
Clinocllore (CHLO 1-30)	(Mg ₅ Al)(Si ₃ Al)O ₁₀ (OH) ₈	680	15 kbar	120	C	0	0	X
Cordierite	Mg ₂ Al ₄ Si ₅ O ₁₈ ·nH ₂ O	810	1 kbar	190-240	M	X	X	0
Enstatite	MgSiO ₃	810	1 kbar	120-340	M	X	X	0
Orthopyroxene (OPX 4-2)	(Mg ₂ Si ₂ O ₆) _{0.92} (MgAl ₂ Si ₆) _{0.08}	1350	15 kbar	98	C	0	0	X
Forsterite	Mg ₂ SiO ₄	800	1 kbar	96-340	M	X	0	0
Forsterite	Mg ₂ SiO ₄	1350	1 atm	216	C	0	0	X
Spinel	MgAl ₂ O ₄	800	1 kbar	240-360	M	0	X	0
Spinel	MgAl ₂ O ₄	1350	1 atm	278	C	0	0	X

X = phase present; 0 = phase absent; * Laboratory designations: M = University of Maine; C = University of Chicago

Each reaction was investigated with starting mixtures that contained equal proportions of the low- and high-temperature assemblage. Typically 5–10 mg of starting mixture was sealed with excess distilled water (25–40 wt%) in a Au or Pt capsule. Successful experiments were evidenced by the constancy of the capsule weight before and after each run and by the appearance of water upon opening the capsule. Reaction direction could be discerned by comparing X-ray diffractometer patterns of the starting mixtures and of the run products. Changes of at least 20% in the relative peak heights were required to indicate a significant change in the modal abundance of the phases. Microscopic examination of experimental products was used to confirm the X-ray diffraction results but was of limited use in determining reaction directions owing to the fine grain size of reactants and products.

Analytical techniques

Unit-cell parameters were obtained using two different procedures. At the University of Maine, cell parameters for all phases, except cordierite, were obtained from X-ray powder-diffraction patterns obtained with an Enraf-Nonius Fr 552 Guinier camera using CuK α radiation and an internal standard of CaF₂

[Baker, lot 91548, $a = 5.4620(5)$ Å] calibrated against diamond ($a = 3.56703$ Å, Robie et al., 1967). Unit-cell refinements were obtained with the least-squares program of Appleman and Evans (1973). Cordierite was refined from a powder-diffraction pattern obtained with an 11.46-cm Debye-Scherrer camera using CuK α radiation and an internal standard of BaF₂ [$a = 6.1971(2)$ Å]. At the University of Chicago, cell parameters were obtained from X-ray diffractometer scans made on a Norelco diffractometer (CuK α radiation) at a scanning rate of $\frac{1}{8}^{\circ}2\theta/\text{min}$ and using corundum as an internal standard. The corundum was annealed Al₂O₃ (Fisher, lot 533145) having the hexagonal parameters $a = 4.7593(3)$ Å and $c = 12.991(1)$ Å, which was calibrated against NBS Standard Reference Material 640 (Si, $a = 5.43088$ Å). Unit-cell refinements were made using the least-squares program of Burnham (1962).

RESULTS

Characterization of Mg-chlorite

Although previous attempts at synthesizing Mg-chlorite have been fairly successful, they have not yielded consistent values for the unit-cell parameters of clinocllore or for the variation in unit-cell parameters as a function of the Al content of chlorite. For example, Figure 2 shows a comparison of c parameters for clinocllore synthesized by Bird and Fawcett (1973), Chernosky (1974), McOnie et al. (1975), Staudigel and Schreyer (1977), and this study. Part of the discrepancy could be attributable to differences in the techniques of unit-cell refinement (i.e., type of instrument, number of peaks used, choice of indices, etc.), but part of it could be caused by genuine differences in chlorite composition arising from incomplete yields of synthetic chlorite. In this study, chlorite synthesized over a range of bulk compositions was carefully examined for extraneous phases using the petrographic microscope, which could be used very effectively for detecting trace amounts of forsterite, orthopyroxene, spinel, and cordierite.

Earlier attempts at calibrating the unit-cell parameter (c in particular) of synthetic chlorite as a function of composition have indicated that c decreases as the Al content increases but previous workers have disagreed on the mag-

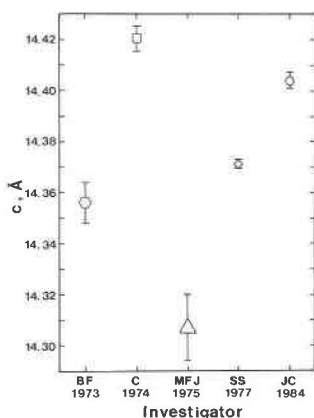


Fig. 2. Values of c parameter of clinocllore synthesized by various investigators: BF = Bird and Fawcett (1973); C = Chernosky (1974); MFJ = McOnie et al. (1975); SS = Staudigel and Schreyer (1977); JC = this study.

Table 3. Synthesis conditions for chlorite on the join $Mg_5Si_3Al_2O_{10}(OH)_8$ - $Mg_{4.6}Si_{2.6}Al_{2.8}O_{10}(OH)_8$

Experiment no.	Lab*	Bulk** composition (x)	P (kb)	T (°C)	Duration (hours)	Products
Ch1-1	M	1.0	3.0	647(3)	1632	Ch1
Ch1-2	M	1.0	3.0	679(3)	2040	Ch1 + trace Fo, Cord & Ta
Ch1-3	M	1.0	3.0	703(2)	2232	Ch1 + minor Fo, Cord & Ta
Ch1-4	M	1.0	3.0	723(5)	2136	Ch1 + moderate Fo, Cord & Ta
CHLO 1-18	C	1.0	14.0	650(5)	51	Ch1
CHLO 1-25	C	1.0	14.0	675(5)	49	Ch1
CHLO 1-13	C	1.0	14.0	700(5)	24	Ch1 + trace Fo?
CHLO 1-26	C	1.0	14.0	730(5)	26	Ch1 + trace Fo + Opx
CHLO 1-17	C	1.0	14.0	765(5)	23	Ch1 + minor Fo
CHLO 1-29	C	1.0	14.0	765(5)	48	Ch1 + minor Fo + Opx?
CHLO 1-23a	C	1.0	14.0	765(5)	102/97	Ch1 + minor Fo
CHLO 1-23b	C	1.0	14.0	765(5)	102/97	Ch1 + minor Fo + Opx
CHLO 1-3	C	1.0	14.0	815(5)	76/27/42	Ch1 + minor Fo + Opx
CHLO 1-27	C	1.0	14.0	820(5)	54	Ch1 + moderate Fo + Opx
CHLO 1-12	C	1.0	14.0	700/820(5)	45/37	Ch1 + moderate Fo + Opx?
CHPR 6-10	C	1.0	14.0	850(5)	47/87	Ch1 + moderate Fo + Opx
Ch1-8	M	1.2	3.0	647(3)	1632	Ch1
Ch1-9	M	1.2	3.0	679(3)	2040	Ch1 + trace Fo, Cord & Ta
Ch1-10	M	1.2	3.0	703(2)	2232	Ch1 + trace Fo, Cord & Ta
Ch1-11	M	1.2	3.0	723(5)	2136	Ch1 + trace Fo, Cord & Ta
Ch1-5	M	1.4	3.0	647(3)	1632	Ch1
Ch1-6	M	1.4	3.0	679(3)	2040	Ch1 + trace Fo, Cord, Ta & Sp
Ch1-7	M	1.4	3.0	703(2)	2232	Ch1 + moderate Fo, Cord, Ta & Sp

* Laboratory designations: M = University of Maine; C = University of Chicago
 ** Aluminum contents are represented by x in the formula: $(Mg_{6-x}Al_x)(Si_{4-x}Al_x)O_{10}(OH)_8$
 † Numbers in parentheses represent two standard deviations from the calculated mean temperatures to their immediate left. Abbreviations: Ch1 = chlorite; Fo = forsterite; Cord = cordierite; Opx = orthopyroxene; Ta = talc; Sp = spinel

nitude and absolute value of this decrease (Fig. 3). In Figure 3, we present a calibration line for the *c* parameter of chlorite synthesized from the bulk compositions *X* = 1.0, 1.2, and 1.4, where *X* designates the number of Al cations in the formula $(Mg_{6-x}Al_x)(Si_{4-x}Al_x)O_{10}(OH)_8$. This line is based on the unit-cell refinements (Table 4) of the purest chlorite syntheses in Table 3 (nos. Ch1-1, -8, -5), namely those chlorites that have no extraneous phases observable under the microscope and that display constancy in their *c* parameters (discussed below). The line obtained in this study is in excellent agreement with that of Shirozu and Momoi (1972) but differs from the curves

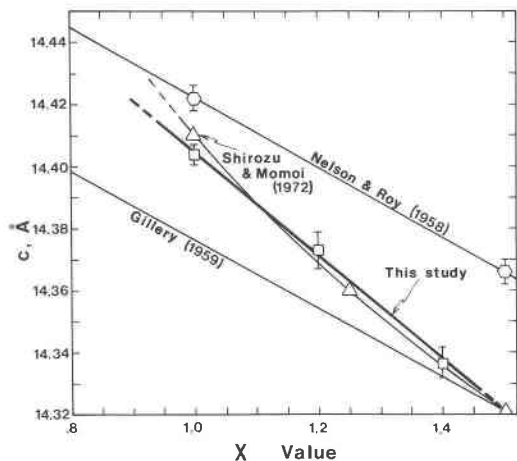


Fig. 3. Calibration curves of *c* as a function of chlorite composition for chlorite synthesized in the system H_2O - MgO - Al_2O_3 - SiO_2 . *X* refers to the Al cations in the formula $(Mg_{6-x}Al_x)(Si_{4-x}Al_x)O_{10}(OH)_8$.

of Nelson and Roy (1958) and Gillery (1959) in both slope and absolute position. Nelson and Roy (1958) and Gillery (1959) apparently did not consider the effects that minor amounts of impurities would have on the composition of synthetic chlorite and thus failed to make the corrections that were made by Shirozu and Momoi (1972).

It was first reported by Jenkins (1980) that chlorite synthesized from a fixed bulk composition and at a given pressure displayed a systematic change in its *c* parameter as a function of the synthesis temperature. This change in *c* is shown in Figure 4, which is based on the data in Tables 3 and 4 for chlorite synthesized at 14 kbar. There is little change in the *c* value of chlorite synthesized below

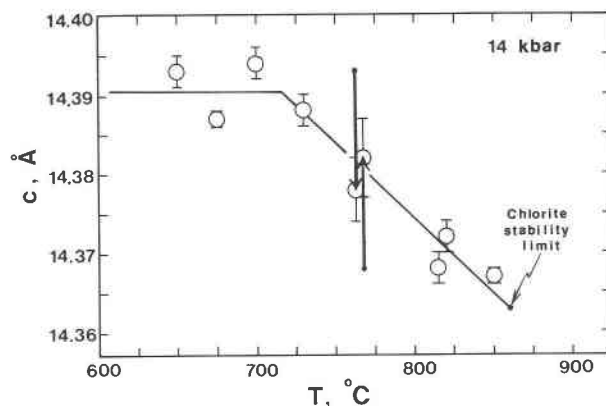


Fig. 4. Values of *c* parameter of chlorite synthesized at 14 kbar ($P_{H_2O} = P_{total}$) from clinocllore bulk composition. Bold arrows indicate re-equilibration of chlorite from an initial *c* at the tail of the arrow to a final *c* at the tip of the arrow. Upper stability of chlorite from Fig. 8.

Table 4. Unit-cell parameters, volumes, and measured d_{004} values for synthetic chlorite

Experiment no.	Bulk composition (x)	a* (Å)	b (Å)	c (Å)	V (Å ³)	d ₀₀₄ ** (Å)
Ch1-1	1.0	5.319(1)	9.215(1)	14.404(3)	700.69(15)	3.576(4)
Ch1-2	1.0	5.320(1)	9.217(1)	14.410(2)	701.18(12)	3.576(2)
Ch1-3	1.0	5.319(1)	9.215(1)	14.388(2)	699.78(12)	3.572(2)
Ch1-4	1.0	5.320(1)	9.215(1)	14.377(3)	699.39(14)	3.570(4)
CHLO 1-18	1.0	5.319(1)	9.218(2)	14.392(3)	700.15(19)	3.573(2)
CHLO 1-18	1.0	5.320(1)	9.211(2)	14.393(2)	699.97(17)	---
CHLO 1-25	1.0	5.318(1)	9.217(3)	14.387(1)	699.95(21)	---
CHLO 1-13	1.0	5.322(1)	9.204(3)	14.394(2)	699.70(19)	---
CHLO 1-26	1.0	5.320(1)	9.215(3)	14.388(2)	700.07(18)	---
CHLO 1-17	1.0	5.320(1)	9.211(2)	14.384(1)	699.50(13)	---
CHLO 1-29	1.0	5.322(1)	9.214(1)	14.397(3)	700.53(14)	3.573(2)
CHLO 1-23a	1.0	5.319(4)	9.219(6)	14.378(4)	699.72(46)	---
CHLO 1-23b	1.0	5.318(3)	9.216(5)	14.382(5)	699.64(36)	---
CHLO 1-3	1.0	5.318(2)	9.208(4)	14.368(2)	698.26(26)	---
CHLO 1-27	1.0	5.318(1)	9.211(1)	14.376(2)	698.75(11)	3.567(2)
CHLO 1-12	1.0	5.320(2)	9.213(2)	14.372(2)	699.02(20)	---
CHPR 6-10	1.0	5.318(1)	9.205(2)	14.367(1)	697.99(14)	---
Ch1-8	1.2	5.319(1)	9.213(4)	14.373(6)	698.87(40)	3.562(1)
Ch1-9	1.2	5.315(2)	9.200(5)	14.377(7)	697.63(49)	3.563(3)
Ch1-10	1.2	5.317(1)	9.210(2)	14.373(3)	698.51(19)	3.566(1)
Ch1-11	1.2	5.320(1)	9.213(1)	14.375(2)	699.15(11)	3.568(3)
Ch1-5	1.4	5.317(1)	9.208(2)	14.337(5)	698.49(27)	3.556(3)
Ch1-6	1.4	5.317(1)	9.207(3)	14.335(8)	696.13(43)	3.557(3)
Ch1-7	1.4	5.319(1)	9.210(1)	14.361(3)	697.96(15)	3.561(3)

* Figures in parentheses following unit cell parameters represent the estimated standard deviation in terms of least units cited for the value to their immediate left; the uncertainties represent precision only.

** d_{004} of chlorite was obtained on chlorites refined at the University of Maine by averaging 6-8 diffractometer scans; the uncertainty represents two standard deviations about the mean value.

about 700°C. Above 700°C there is a distinct decrease in c with a concomitant appearance of orthopyroxene and forsterite which gradually increase in modal abundance with increasing temperature. Both the decrease in c and the appearance of orthopyroxene and forsterite suggest that chlorite synthesized above 700°C is more aluminous than clinocllore. The constancy of the c values and the absence of coexisting phases below 700°C suggests that pure clinocllore can only be synthesized below this temperature (at 14 kbar).

The behavior of chlorite displayed in Figure 4 does not appear to be an artifact of the synthesis technique as shown by the results of a re-equilibration experiment (bold arrows). In this experiment, one chlorite was synthesized at 815°C and one at 650°C; both were analyzed and resealed with excess H₂O in separate capsules, placed side-by-side in the same experimental assemblage, and re-equilibrated at 765°C and 14 kbar (runs CHLO 1-23a and b in Table 3). Both chlorites exhibited a significant shift from their initial c values toward those obtained from the synthesis

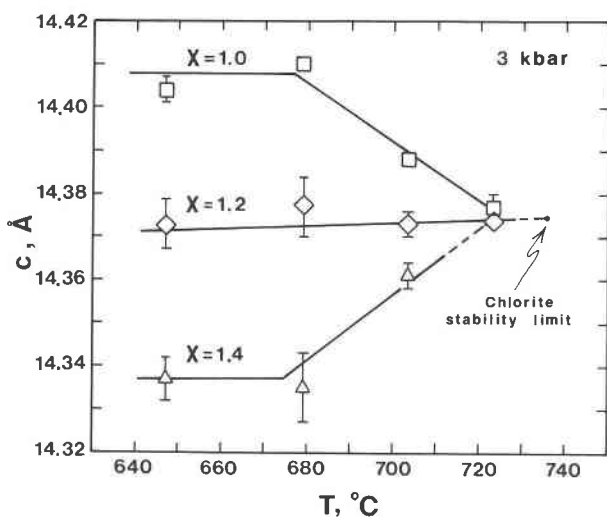


Fig. 5. Values of c parameter of chlorite synthesized at 3 kbar ($P_{\text{H}_2\text{O}} = P_{\text{total}}$) from bulk compositions corresponding to $X = 1.0$, 1.2, and 1.4 (X defined in Table 1). Upper stability of chlorite from Fig. 8.

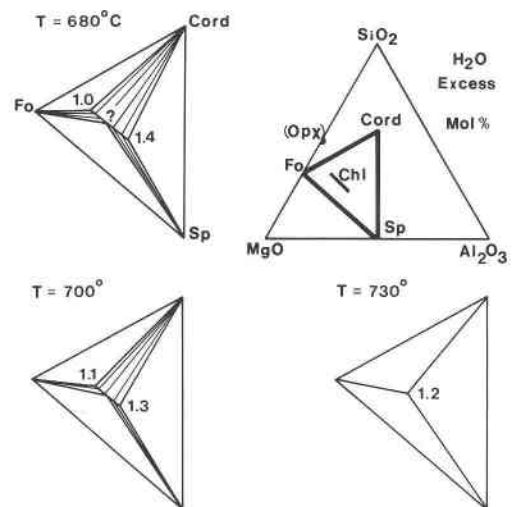


Fig. 6. Schematic representation of the change in chlorite composition with increasing temperature at a constant pressure ($=P_{\text{H}_2\text{O}}$) of 3 kbar. Numbers refer to the X parameter of chlorite defined in Table 1. Abbreviations in Table 1.

Table 5. Phase-equilibrium data for Reactions A, B, and C

Experiment no.	T (°C)	P _{H₂O} (kbar)	Duration (hours)	Comments*	Extent of Reaction**
Reaction A: Chl + Opx = Fo + Cord + H ₂ O					
13	595(3)	0.5	1464	Chl (+)Opx (-)Fo (-)Cord (-)Ta (+) [†]	M
22	612(2)	0.5	1128	Chl (-)Opx (-)Fo (+)Cord (+)	M
15	622(2)	0.5	1224	Chl (-)Opx (-)Fo (+)Cord (+)	M
16	633(2)	0.5	1176	Chl (-)Opx (-)Fo (+)Cord (+)	M
11	634(2)	1.0	1459	Chl (+)Opx (-)Fo (-)Cord (-)Ta (+)	M
24	660(3)	1.0	1152	Chl (-)Opx (-)Fo (+)Cord (+)	M
18	670(2)	1.0	1176	Chl (-)Opx (-)Fo (+)Cord (+)	M
8	676(3)	1.0	1446	Chl (-)Opx (-)Fo (+)Cord (+)	S
4	615(3)	2.0	1824	Chl (+)Opx (-)Fo (-)Cord (-)Ta (+)	S
6	667(4)	2.0	5064	Chl (+)Opx (+)Fo (-)Cord (-)Ta (+)	S
25	691(3)	2.0	1296	Chl (+)Opx (+)Fo (-)Cord (-)	M
1	695(5)	2.0	1680	Chl (+)Opx (+)Fo (-)Cord (-)	S
9	697(2)	2.0	1459	Chl (-)Opx (-)Fo (+)Cord (+)	M
20	706(3)	2.0	1008	Chl (-)Opx (-)Fo (+)Cord (+)	S
7	717(4)	2.0	1440	Chl (-)Opx (-)Fo (+)Cord (+)	S
3	678(3)	3.0	1800	Chl (+)Opx (-)Fo (-)Cord (-)Ta (+)	S
5	719(4)	3.0	5064	Chl (+)Opx (+)Fo (-)Cord (-)	S
21	734(2)	3.0	1104	Chl (-)Opx (-)Fo (+)Cord (+)	M
2	737(3)	3.0	1800	Chl (-)Opx (-)Fo (+)Cord (+)	S
Reaction B: Chl + Cord = Opx + Sp + H ₂ O					
18	740(3)	3.0	1368	Chl (-)Cord (-)Opx (+)Sp (+)	M
15	733(3)	3.5	1560	Chl (+)Cord (+)Opx (-)Sp (-)	W
10	730(4)	4.0	1488	Chl (+)Cord (+)Opx (-)Sp (-)	S
4	750(6)	4.7	1656	Chl (-)Cord (-)Opx (+)Sp (+)	S
8	722(4)	5.0	1656	Chl (+)Cord (+)Opx (-)Sp (-)Ta (+)	S
9	735(3)	5.0	1560	Chl (+)Cord (+)Opx (-)Sp (-)	S
19	744(2)	5.0	336	Chl (+)Cord (+)Opx (-)Sp (-)	S
11	731(2)	6.0	1128	Chl (+)Cord (+)Opx (-)Sp (-)Ta (+)	S
Reaction C: Chl ≠ Opx + Sp + Fo + H ₂ O					
CHPR 7-6	770(5)	6.1(1)	47	Chl (+)Opx (-)Sp (-)Fo (-)	S
CHPR 7-12	775(2)	6.06(5)	70	Chl (+)Opx (-)Sp (-)Fo (-)	M
CHPR 7-8	780(4)	6.05(5)	65	Chl (-)Opx (+)Sp (+)Fo (+)	W
CHPR 7-7	790(3)	6.0(1)	71	Chl (-)Opx (+)Sp (+)Fo (+)	S
CHPR 7-4	800(3)	6.1(1)	93	Chl (-)Opx (+)Sp (+)Fo (+)	S
CHPR 7-9	800(3)	8.0(1)	24	Chl (+)Opx (-)Sp (+)Fo (-)	S
CHPR 7-13	804(3)	8.0(1)	36	Chl (+)Opx (-)Sp (-)Fo (-)	S
CHPR 7-11	810(3)	8.02(7)	43	Chl (+)Opx (-)Sp (-)Fo (-)	M
CHPR 7-10	820(3)	8.09(7)	45	Chl (-)Opx (+)Sp (+)Fo (+)	S

* + = Growth of phase; - = Diminution of phase

** Symbols S, M, and W are qualitative estimates of the extent of reaction and represent greater than 75%, 75-25%, and less than 25% reaction, respectively.

† Ta = talc; other abbreviations same as in Fig. 1.

runs, which gives strong evidence for the reversibility of this process.

A similar study of the change in the chlorite *c* parameter as a function of temperature was conducted at 3 kbar and over a range of bulk compositions. The results of this study (Tables 3 and 4) are plotted in Figure 5. For *X* = 1.0 (pure clinocllore), the change in *c* is nearly identical to that in Figure 4, namely, there is a distinct decrease in *c* and a concomitant appearance of coexisting Al-poor phases at and above 680°C. Chlorite synthesized from the bulk composition *X* = 1.2 shows very little change in *c* and has only trace amounts of coexisting phases. Chlorite synthesized from the bulk composition *X* = 1.4 displays a distinct increase in *c* and coexists with the Al-rich phase spinel at and above 680°C. Thus all three curves display a convergence toward a single *c* value and, presumably, toward the same composition near the stability limit of chlorite at 3 kbar.

A comparison of Figures 4 and 5 shows that the *c* parameter of chlorite at its maximum thermal stability is

essentially the same (14.363 vs. 14.367 Å) for the bulk compositions examined in this study. Based on Figure 3, this value of *c* corresponds to *X* = 1.2, which is a chlorite that is slightly more aluminous than clinocllore. This particular composition is in accord with the experimental work of Fawcett and Yoder (1966) and Fleming and Fawcett (1976), who found that Mg-chlorite at its maximum stability in the presence of quartz is more aluminous than clinocllore and falls within the range of Al contents that is optimal for relieving the structural misfit between the tetrahedral and trioctahedral sheets in the chlorite structure (e.g., Bradley, 1959; Zen, 1960). Moreover, the similarity in chlorite composition over such a wide pressure interval (3-14 kbar) suggests that the composition of chlorite is constant (i.e., *X* = 1.2) at its upper thermal stability.

An alternative way of representing the change in chlorite composition described above is with a series of isothermal projections from H₂O onto the ternary plane MgO-Al₂O₃-SiO₂. Figure 6 is a schematic representation of the compositional limit of chlorite as the temperature increases

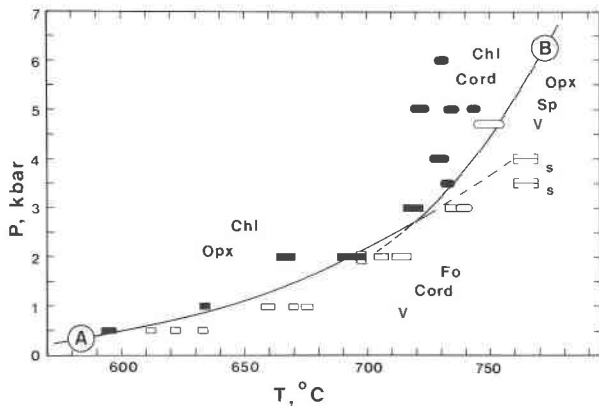


Fig. 7. Experimental data for Reactions A (square symbols) and B (rounded symbols) in the text. Abbreviations in Table 1. Filled and open symbols represent growth of the low-temperature and high-temperature assemblage, respectively. Brackets labeled S are reversals for Reaction B by Seifert (1974). Curves are taken from Fig. 8.

from 680°C to the upper thermal stability of chlorite at 3 kbar (730°C). The composition of chlorite in equilibrium with forsterite and spinel has been approximated as indicated by the question mark. A similar set of diagrams could be constructed for pressures above 3 kbar, using orthopyroxene in place of cordierite, where the final or terminal chlorite composition would again correspond to $X = 1.2$.

Identification of 7-Å phases

Since the pioneering study of Yoder (1952), considerable effort has been devoted to identifying and determining the stability of "7-Å chlorite" or serpentine (lizardite) that could be coexisting with synthetic 14-Å chlorite (Roy and Roy, 1955; Nelson and Roy, 1958; Gillery, 1959; Velde, 1973; Cho and Fawcett, 1986). The identification of serpentine by X-ray diffraction is rather difficult because its basal (001) reflections overlap with those of chlorite. The criterion set forth by Chernosky (1974), who has assigned a reflection with $d = 4.59 \text{ \AA}$ to lizardite, is necessary but not sufficient for the positive identification of a 7-Å phase. Many natural IIb chlorites (14 Å) have X-ray reflections at $d = 4.59\text{--}4.61 \text{ \AA}$ (Shirozu, 1978). Furthermore, this peak is observed in X-ray patterns of chlorite synthesized individually and in reversal mixtures made in this study at temperatures as high as 820°C, which is above the stability of most serpentine phases (e.g., Caruso and Chernosky, 1979). Even with multiple grindings and hydrothermal treatments at 820°C and 14 kbar, this peak persists at about the same intensity. All of these observations suggest the peak at 4.59 \AA belongs to chlorite and not serpentine. Thus if one is to use a single X-ray peak for the identification of 7-Å phases, it should be used in conjunction with either a careful study of relative peak intensities (Yoder, 1952) or an independent technique such as infrared spectroscopy (Shirozu and Ishida, 1982).

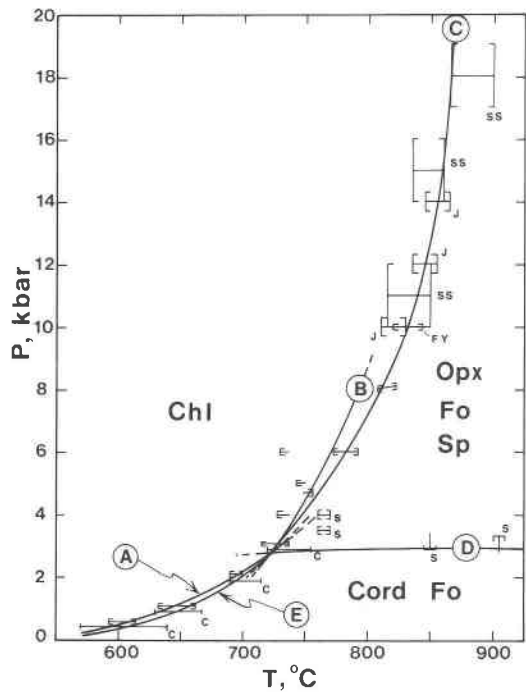


Fig. 8. Univariant curves pertinent to the upper stability of Mg-chlorite in the system $\text{H}_2\text{O-MgO-Al}_2\text{O}_3\text{-SiO}_2$, with excess H_2O , calculated from the experimental brackets shown here. Circled letters refer to reactions in the text. Experimental brackets are from the following sources: Unlabeled = this study; C = Chernosky (1974); FY = Fawcett and Yoder (1966); J = Jenkins (1981); S = Seifert (1974); SS = Staudigel and Schreyer (1977). Abbreviations in Table 1.

Experimental phase equilibria

The maximum thermal stability of chlorite in the presence of orthopyroxene is governed by (endmember) Reaction A. Key experiments delimiting the position of Reaction A are listed in Table 5 and are represented by filled and open symbols corresponding to growth of the low-temperature or high-temperature assemblage, respectively, in Figure 7. Although talc nucleated spontaneously in the lowest-temperature experiments (Table 5), its modal abundance was not sufficient to obscure the phase relations of interest. The appearance of talc is probably caused by the metastability of enstatite and water with respect to talc and forsterite in the lowest-temperature experiments.

The maximum stability of chlorite in the presence of cordierite is governed by (endmember) Reaction B. Experiments pertaining to Reaction B are listed in Table 5 and are plotted in Figure 7. As in Reaction A, talc was observed to nucleate in two of the runs (nos. 8 and 11) but was not present in sufficient amounts to compromise the results. Also shown in Figure 7 are two experimental brackets for Reaction B from Seifert (1974) suggesting that Reaction B lies 10–30° higher in temperature than we have placed it. This discrepancy could be caused by a combination of the markedly shorter run durations used by Seifert (1974) (165–283 h) and the proximity of these

Table 6. Volumes and heat-capacity equations used in Equation 3

Phase	$V_{298\text{ K}}^1$ cm ³ /mole	a	b ($\times 10^{-2}$)	c ($\times 10^6$)	d ($\times 10^3$)	e ($\times 10^{-5}$)
Clinchlore	210.9(1)*	807.8 [‡]	12.81	-17.984	-1.5458	-2.1857
Cordierite	234.3(2)*	821.34 [‡]	4.3339	-8.2112	-5.003	---
Enstatite	31.34(2)**	172.96 ^{§§}	-0.015538	-0.7086	-1.4316	---
Forsterite	43.67(1) [†]	227.98 [§]	0.34139	-0.89397	-1.7446	---
Spinel	39.75(1) [†]	222.91 [§]	0.61267	-1.6857	-1.5512	---
H ₂ O (steam)	---	7.3680 [§]	2.7468	-0.22316	0.36174	-0.48117

Coefficients to the heat-capacity expressions apply to the relation: $C_p = a + bT + c/T^2 + d/\sqrt{T} + e(T^2)$ J/mol·K

* This study
** Ganguly and Ghose (1979) †† Estimated by summing C_p data for brucite, talc, and the difference between
† Charlu et al. (1975) gehlenite and akermanite, from Robie et al. (1978)
§ Robie et al. (1978) §§ Krupka et al. (1979), refitted to a 4-term polynomial (Holland, 1981)

experiments to the metastable extension of Reaction A (where chlorite could grow metastably at the expense of cordierite). In any case, it is believed that the results of the present study represent a closer approach to equilibrium conditions than do the results of Seifert (1974).

The upper thermal stability of chlorite above about 3 kbar is governed by (endmember) Reaction C. Experimental results pertaining to Reaction C at 6 and 8 kbar are listed in Table 5 and are shown in Figure 8 along with experimental results obtained at 10 kbar by Fawcett and Yoder (1966), at 11–18 kbar by Staudigel and Schreyer (1977), and at 10–14 kbar by Jenkins (1981).

THERMODYNAMIC CALCULATIONS

There are two main objectives to the thermodynamic analyses performed here: (1) to determine whether or not the experimental brackets for a particular reaction are consistent with each other and (2) to determine if the entire set of experimental brackets for all of the reactions permit construction of an array of univariant curves that converge on an invariant point. The approach to both of these objectives lies in the thermodynamics of univariant reactions, which are briefly reviewed below.

At each value of P and T along a univariant curve, the following relationship must be obeyed:

$$\Delta G_{P,T} = 0 = \Delta G_{P_0,T_0}^0 - \int_{T_0}^T \Delta S_{P_0,T}^0 dT + \int_{P_0}^P \Delta V_{P,T}^{\text{solids}} dP + nRT \ln f_{P,T}^{\text{H}_2\text{O}} + RT \ln K_a \quad (1)$$

where P_0 and T_0 are the reference pressure (taken here as 1 bar) and temperature, respectively, the standard state is that of unit activity for the pure solid phase at P and T , and the ideal gas at 1 bar and T for H₂O. If heat-capacity data are available for all of the phases, then the second term on the right-hand side can be expanded to give

$$\begin{aligned} \int_{T_0}^T \Delta S_{P_0,T}^0 dT &= \int_{T_0}^T \left[\Delta S_{P_0,T_0}^0 + \int_{T_0}^T \frac{\Delta C_p}{T} dT \right] dT \\ &= \Delta S_{P_0,T_0}^0 (T - T_0) \\ &\quad + \int_{T_0}^T \left[\int_{T_0}^T \frac{\Delta C_p}{T} dT \right] dT. \end{aligned} \quad (2)$$

Substituting Equation 2 into Equation 1 and rearranging gives the relation

$$\begin{aligned} -\Delta G_{P_0,T_0}^0 + \Delta S_{P_0,T_0}^0 (T - T_0) \\ &= - \int_{T_0}^T \left[\int_{T_0}^T \frac{\Delta C_p}{T} dT \right] dT + \int_{P_0}^P \Delta V_{P,T}^{\text{solids}} dP \\ &\quad + RT \ln f_{P,T}^{\text{H}_2\text{O}} + RT \ln K_a \\ &= G'. \end{aligned} \quad (3)$$

The terms on the right-hand side of Equation 3 are combined into a single term called G' , which will be treated as a constant at any given P and T . By doing this, we are asserting that the heat capacities, volumes, H₂O fugacities, and activities are better known than the entropies or Gibbs free energies of the phases and that these latter two quantities are viewed as unknowns or variables. The accuracy of this assertion is certainly debatable; nevertheless, this approach is adopted here in order to avoid a lengthy discussion of each datum that enters into the thermodynamic calculations and to simplify attaining the objectives of this study.

Evaluation of Equation 3 requires knowledge of the heat capacities and volumes of the pure solids, water fugacity, and activity-composition relations for the phases that have variable compositions (i.e., chlorite, cordierite, and orthopyroxene). One simplification that will be made is that

$$\int_{T_0}^T \Delta V_{P,T}^{\text{solids}} dP = (\Delta V_{1\text{ bar},298\text{ K}}^{\text{solids}}) \Delta P$$

(i.e., $V^{\text{solids}} = \text{constant}$), which is generally thought to introduce insignificant errors over a range of 10–20 kbar (Helgeson et al., 1978, p. 32). Heat-capacity expressions and volumes used in this study are listed in Table 6. Note that the heat-capacity expression for enstatite has been refitted to a 4-term polynomial expression to provide a reasonable extrapolation of the heat capacities beyond the temperature at which they were measured. Water fugacities below 10 kbar were taken from Burnham et al. (1969) and above 10 kbar from Delany and Helgeson (1978). Of

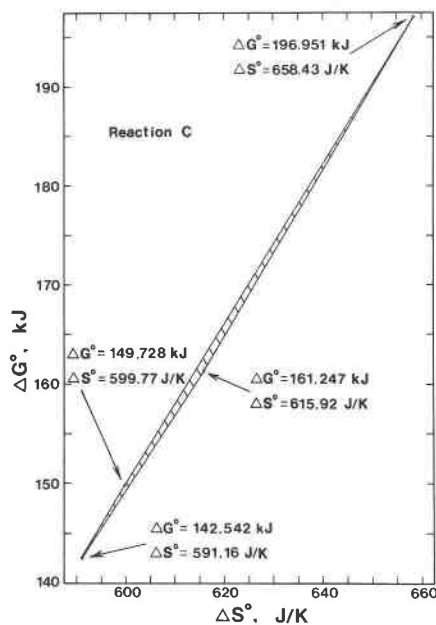


Fig. 9. Graphical solution to the linear programming analysis of Reaction C in the text. Shaded area is the region of feasible ΔG° and ΔS° of reaction values satisfying all of the experimental brackets.

the phases considered here in the system $\text{H}_2\text{O}-\text{MgO}-\text{Al}_2\text{O}_3-\text{SiO}_2$, only chlorite, cordierite, and orthopyroxene experience any significant change in composition. Although chlorite can assume variable Al_2O_3 contents, it was argued above that the composition of chlorite remains essentially constant, as $(\text{Mg}_{4.8}\text{Al}_{1.2})(\text{Si}_{2.8}\text{Al}_{1.2})\text{O}_{10}(\text{OH})_8$, at its upper thermal stability. It will suffice for the present purposes to fix the activity of $(\text{Mg}_5\text{Al})(\text{Si}_3\text{Al})\text{O}_{10}(\text{OH})_8$ in chlorite ($a_{\text{Chl}}^{\text{Chl}}$) at 0.8, which is equivalent to treating chlorite as an ideal mixture of the components $(\text{Mg}_5\text{Al})(\text{Si}_3\text{Al})\text{O}_{10}(\text{OH})_8$ and $(\text{Mg}_3\text{Al}_2)(\text{Si}_2\text{Al}_2)\text{O}_{10}(\text{OH})_8$. The primary compositional variable for cordierite in this system is its H_2O content. Recent thermodynamic treatments have sought to characterize Mg-cordierite as an ideal mixture of hydrous and anhydrous cordierite endmembers (Newton and Wood, 1979), as the solution of H_2O into $\text{Mg}_2\text{Al}_4\text{Si}_5\text{O}_{18}$ according to Henry's law (Martignole and Sisi, 1981), and as an ideal one-site mixture of H_2O in $\text{Mg}_2\text{Al}_4\text{Si}_5\text{O}_{18}$ (Lonker, 1981). None of these activity models is in complete agreement with the experimental data on cordierite. However, we have chosen the Newton and Wood (1979) model for determining the activity of $\text{Mg}_2\text{Al}_4\text{Si}_5\text{O}_{18}$ in hydrous cordierite ($a_{\text{Cord}}^{\text{Cord-H}_2\text{O}}$) both for its simplicity and because it is based on the data of Mirwald and Schreyer (1977) which were obtained in a P - T range where equilibrium water contents are thought to be quenchable (Medenbach et al., 1980). Orthopyroxene in this system consists of enstatite with variable amounts of Al_2O_3 . To a close approximation, the Al_2O_3 content of orthopyroxene in each reaction is fixed by the phases forsterite and spinel. Gasparik and Newton (1984) determined the compositions of orthopyroxene in equilibrium with forsterite and spinel

and found that the activity of $\text{Mg}_2\text{Si}_2\text{O}_6$ in orthopyroxene ($a_{\text{En}}^{\text{Opx}}$) is quite accurately expressed by the ideal activity expression

$$a_{\text{En}}^{\text{Opx}} = (X_{\text{Mg}}^{\text{M2}})(X_{\text{Mg}}^{\text{M1}}), \quad (4)$$

where $X_{\text{Mg}}^{\text{M2}}$ and $X_{\text{Mg}}^{\text{M1}}$ are the mole fractions of Mg on the M2 and M1 octahedral sites, respectively. Using the cation distribution scheme proposed by Wood and Banno (1973), one sees that $X_{\text{Mg}}^{\text{M2}} = 1.0$ and $X_{\text{Mg}}^{\text{M1}} = X_{\text{En}}^{\text{Opx}} = a_{\text{En}}^{\text{Opx}}$. Combining this with the experimental data of Gasparik and Newton (1984), one obtains (T in kelvins; P in bars)

$$a_{\text{En}}^{\text{Opx}} = \frac{1}{k + 1}, \quad (5)$$

where

$$k = \exp \left[\frac{-29190 + 13.42T - 0.18T^{1.5} - \int \Delta V dP}{8.31432T} \right]$$

and

$$\int \Delta V dP = [0.013 + 3.34 \times 10^{-5}(T - 298) - 6.6 \times 10^{-7}P]P.$$

The internal consistency of a set of experimental brackets for a given reaction can be determined by using linear programming (e.g., Gordon, 1973). Each experimental bracket delimits a rectangular area in P - T space (or half of a rectangle in the case of "half-brackets") within which a univariant curve must lie, and the two furthest possible points of each experimental bracket (i.e., a diagonal of a rectangle) define a line in P - T space through which the curve must pass. At either end of this line, one has the thermodynamic relation (from Eq. 3)

$$-\Delta G^\circ + \Delta S^\circ(T - T_0) \geq \text{or} \leq G', \quad (6)$$

which states that the G' value of the univariant boundary must be greater than or equal to or less than or equal to the G' value at either end of the line. In a graphical sense, Equation 6 allows a univariant boundary to pass through any part of an experimental bracket, including the extreme corners, but the boundary cannot lie outside the bracket. Using Equation 6, one can formulate inequality expressions at the extreme corners of each experimental bracket, plot these as straight lines on a graph of ΔG° vs. ΔS° , and shade in the areas that satisfy the inequalities for each expression. If there is an area that satisfies all of the inequalities, then there is a feasible range of values of ΔG° and ΔS° of reaction that satisfies all of the experimental brackets, and the experimental data are said to be internally consistent. If there is no such range of feasible solutions, then the experimental data are inconsistent.

The procedure outlined above was performed on Reactions A, B, and C already discussed above as well as for (endmember) Reaction D,

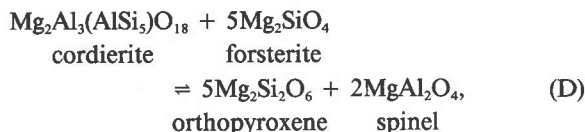


Table 7. Numerical values for the terms composing G' (Eq. 3) for Reactions A-E

Source* and reaction direction**	Bracket diagonal†		G'			
	T (K)	P (kbar)	$\int_{T_0}^T \Delta C_P$ (kJ)	C_P^S (kJ)	$RT \ln K_a^{SS}$ (kJ)	$nRT \ln f_{P,T}^{H_2O}$ (kJ)
Reaction A: 2 Chl + 3 Opx = Cord + 7 Fo + 8 H ₂ O						
JC L	865	0.55	-3.842	52.316	3.050	346.615
R	887	0.45	-3.143	56.253	3.358	348.076
JC L	905	1.05	-7.334	59.559	2.933	394.501
R	936	0.95	-6.636	65.412	3.332	407.031
JC L	963	2.05	-14.319	70.690	2.582	461.248
R	972	1.95	-13.621	72.474	2.825	464.023
JC L	988	3.05	-21.304	75.706	1.926	502.443
R	1009	2.95	-20.606	80.017	2.317	513.427
Reaction B: 5 Chl + Cord = 10 Opx + 7 Sp + 20 H ₂ O						
JC L	1003	3.55	-136.231	145.469	7.155	1309.119
R	1016	2.95	-113.206	150.298	6.369	1294.739
JC L	1015	5.05	-193.793	149.922	8.603	1407.812
R	1029	4.65	-178.444	155.192	7.985	1411.440
Reaction C: Chl = Opx + Fo + Sp + 4 H ₂ O						
JC L	1046	6.11	-39.593	35.642	1.232	302.362
R	1066	5.90	-38.232	37.366	1.215	307.174
JC L	1074	8.14	-52.747	38.063	1.213	330.588
R	1096	8.00	-51.840	40.003	1.192	337.031
FY L	1093	10.1	-65.448	39.737	1.200	353.851
R	1115	9.9	-64.152	41.705	1.178	360.048
JC L	1083	10.3	-66.744	38.853	1.209	351.862
R	1103	9.7	-62.856	40.628	1.190	354.126
SS L	1088	12.0	-77.760	39.294	1.207	366.537
R	1123	10.0	-64.800	42.428	1.171	363.700
JC L	1108	12.3	-79.704	41.075	1.190	375.922
R	1128	11.7	-75.816	42.883	1.168	378.632
SS L	1108	16.0	-103.680	41.075	1.196	402.452
R	1133	14.0	-90.720	43.339	1.170	397.288
JC L	1118	14.3	-92.664	41.976	1.183	394.036
R	1138	13.7	-88.776	43.796	1.162	396.894
SS L	1138	19.0	-123.120	43.796	1.169	434.284
R	1173	17.0	-110.160	47.043	1.128	433.077
Reaction D: Cord + 5 Fo = 2 Sp + 5 Opx						
S L	1118	2.90	-17.328	-19.804	-1.963	-----
R	1183	3.35	-20.016	-22.932	-2.656	-----
S L	1268	2.70	-16.132	-27.315	-4.929	-----
R	1278	3.10	-18.522	-27.867	-4.879	-----
S L	1368	2.40	-14.340	-32.837	-7.233	-----
R	1378	2.90	-17.328	-33.389	-7.123	-----
Reaction E: 5 Chl = 10 Fo + 3 Sp + Cord + 20 H ₂ O						
C L	844	0.51	-13.477	108.518	6.599	834.024
R	913	0.49	-12.948	135.839	7.421	910.793
C L	904	1.02	-26.953	132.164	6.777	981.802
R	940	0.98	-25.896	147.181	7.260	1026.631
C L	962	2.04	-53.907	156.658	6.391	1150.941
R	988	1.96	-51.793	168.129	6.807	1184.836
C L	994	3.06	-80.860	170.803	5.860	1266.314
R	1018	2.94	-77.690	181.720	5.184	1297.318

* Sources of experimental data: C = Chernosky (1974); FY = Fawcett and Yoder (1966); JC = This study; S = Seifert (1974); SS = Staudigel and Schreyer (1977).
 ** Reaction direction: L = left-hand assemblage grew at the expense of the right-hand assemblage; R = (vice versa).
 † Experimental brackets incorporate the maximum uncertainties cited by each investigator. See text for further discussion.
 § This is the numerical value for the term

$$-\int_{T_0}^T \left[\int_{T_0}^T \frac{\Delta C_P}{T} dT \right] dT$$

§§ K_a expressions in Table 8.

Table 8. Equilibrium constants for Reactions A-E

Reaction	K_a^*
A	$\left(\frac{a_{Cord-H_2O}^0}{a_{Cord}^{Chl}} \right) / \left(\frac{a_{Chl}^{Chl}}{a_{Clino}^{Chl}} \right)^2 \left(\frac{a_{Opx}^{Opx}}{a_{En}^{Opx}} \right)^3$
B	$\left(\frac{a_{Opx}^{Opx}}{a_{En}^{Opx}} \right)^{10} / \left(\frac{a_{Chl}^{Chl}}{a_{Clino}^{Chl}} \right)^5 \left(\frac{a_{Cord-H_2O}^0}{a_{Cord}^{Cord}} \right)^2$
C	$\left(\frac{a_{Opx}^{Opx}}{a_{En}^{Opx}} \right) / \left(\frac{a_{Chl}^{Chl}}{a_{Clino}^{Chl}} \right)$
D	$\left(\frac{a_{Opx}^{Opx}}{a_{En}^{Opx}} \right)^5 / \left(\frac{a_{Cord-H_2O}^0}{a_{Cord}^{Cord}} \right)$
E	$\left(\frac{a_{Cord-H_2O}^0}{a_{Cord}^{Cord}} \right) / \left(\frac{a_{Chl}^{Chl}}{a_{Clino}^{Chl}} \right)^5$

* $a_{Cord-H_2O}^0$ = activity of $Mg_2Al_3(AlSi_5)O_{18}$ in hydrous cordierite
 a_{Chl}^{Chl} = activity of $(Mg_5Al)(Si_3Al)O_{10}(OH)_8$ in chlorite
 a_{En}^{Opx} = activity of $Mg_2Si_2O_6$ in orthopyroxene

which was investigated by Chernosky (1974). The experimental brackets reported in Table 5 for Reactions A, B, and C and in the literature for Reactions C, D, and E were "expanded" to their greatest possible P - T range by including the reported uncertainties in the measurement of pressure and temperature. These expanded brackets are shown in Figures 7 and 8. It should be noted that the 1000 and 1100°C brackets for Reaction D from Seifert (1974) are not shown in Figure 8 but were included in the calculations (Table 7). The corners of each bracket farthest from the anticipated location of the univariant boundary were identified, and the value of G' calculated at these corners. The P , T , and thermodynamic values entering into the calculation of G' at the diagonal corners of each bracket are listed in Table 7, and the equilibrium constant for each reaction is defined in Table 8. Inequality expressions were formulated using Equation 6 and the data in Table 7, and the range of feasible values of ΔG^0 and ΔS^0 of reaction for each reaction was determined both graphically and analytically using a linear programming computer program modified after that of Frazer (1968). The results of linear programming reveal that the experimental brackets for each reaction taken separately are internally consistent for all five reactions. Reaction C is shown in Figure 9 as an example of the graphical solution to the linear programming analysis. Notice that the area of feasible ΔG^0 and ΔS^0 values is a very slender trapezium whose four corners are labeled on the figure. The maximum and minimum values of ΔG^0 and ΔS^0 for the five individual reactions are listed in Table 9. Notice that Reaction B has a feasible range of values with no upper limit.

It is a relatively simple task to perform linear programming on the experimental brackets of all five reactions simultaneously to determine if they are consistent with one another and with an array of univariant curves about an invariant point. Two additional constraints, namely that the summation of ΔG^0 and ΔS^0 for all reactions about an invariant point be zero (Gordon, 1973), were added to the linear programming problem. Given the stoichiometry of Reactions A, B, C, D, and E as written in this study, these summations are

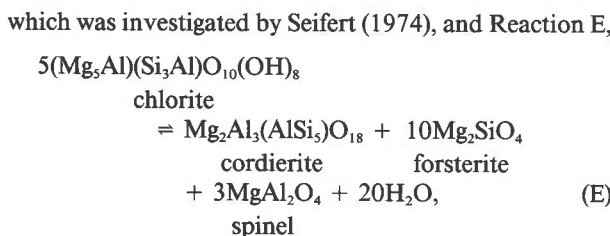


Table 9. ΔG° and ΔS° values at 298 K and 1 bar for Reactions A–E

Reaction	Individual reactions*				Invariant point array**			
	ΔG° (kJ)		ΔS° (J/K)		ΔG° (kJ)		ΔS° (J/K)	
	max.	min.	max.	min.	max.	min.	max.	min.
A	491.798	298.862	1521.80	1229.28	491.798	308.077	1521.80	1245.53
B	∞	590.488	∞	2717.73	953.735	590.491	3214.65	2717.73
C	196.951	142.542	658.43	591.16	196.951	196.951	658.43	658.43
D	3.478	-20.024	-47.60	-72.10	-20.024	-20.024	-72.10	-72.10
E	1305.122	568.681	3832.24	2743.35	915.910	736.387	3225.99	3005.35

* Maximum and minimum values for each individual reaction obtained via linear programming
** Maximum and minimum values for all reactions subject to the stoichiometric relationship that $A - B - 2C + 3D + E = 0$; obtained via linear programming

$$\Delta G_A^\circ - \Delta G_B^\circ - 2\Delta G_C^\circ + 3\Delta G_D^\circ + \Delta G_E^\circ = 0 \quad (7a)$$

$$\Delta S_A^\circ - \Delta S_B^\circ - 2\Delta S_C^\circ + 3\Delta S_D^\circ + \Delta S_E^\circ = 0. \quad (7b)$$

Applying these two additional constraints to the data, one can determine via linear programming that there is a range of feasible values of ΔG° and ΔS° for all five reactions and that the data are internally consistent with an array of univariant curves about an invariant point. The maximum and minimum values of ΔG° and ΔS° for each reaction in this array are given in the last four columns of Table 9.

An array of univariant curves has been calculated for the experimental brackets in Figures 7 and 8 using Equation 3 and the average of the ΔG° and ΔS° values in the last four columns of Table 9. The calculated invariant point lies at $720 \pm 10^\circ\text{C}$ and 2.75 ± 0.30 kbar (Fig. 8), which is slightly lower in P and T conditions than the invariant point determined by Fawcett and Yoder (1966) ($765 \pm 10^\circ\text{C}$, 3.25 ± 0.25 kbar). The close proximity of Reactions A, B, C, and E reflects a property that might be coined "dehydration degeneracy." Each of these reactions involves the release of 4 mol H_2O per 1 mol chlorite, which dominates the entropy and free-energy change of the reactions. The result is that these boundaries nearly coincide.

DISCUSSION

Current estimates of the thermochemical parameters ΔG_f° , ΔH_f° , and ΔS_f° for pure clinocllore ($X = 1.0$) show considerable scatter (Table 10). The experimental phase equilibria and crystallochemical data presented here should provide the best determinations to date.

Reactions A, B, C, and E deal explicitly with the clinocllore component in chlorite and, therefore, allow the extraction of thermochemical data for clinocllore from

the ΔG° and ΔS° values reported in Table 9. It is stressed, however, that an accurate assessment of the equilibrium constant is necessary for this task and that one must choose experimental data involving phases with well-known activity-composition relations. This immediately rules out all reactions involving cordierite, whose hydration state and activity-composition relations are widely debated, and leaves Reaction C as the best candidate. From Table 8 one can see that there are only two terms in Reaction C to consider: $a_{\text{En}}^{\text{Opx}}$ and $a_{\text{Cln}}^{\text{Chl}}$. The former term is well known from such studies as Gasparik and Newton (1984) where the Al_2O_3 content of orthopyroxene in equilibrium with forsterite and spinel is dealt with explicitly. The latter term, however, has only been approximated in this study ($a_{\text{Cln}}^{\text{Chl}} \cong 0.8$), with no independent experimental evidence to demonstrate the validity of this approximation. Fortunately, the energetics of Reaction C are such that any reasonable choice of $a_{\text{Cln}}^{\text{Chl}}$ (i.e., 0.65–1.0) produces only trivial changes in the derived values of ΔG_f° (± 1.5 kJ/mol) and ΔS_f° (± 4 J/K·mol).

The derivation of ΔG_f° and ΔS_f° for clinocllore follows directly from the values of ΔG° and ΔS° for Reaction C that were obtained in the previous section (Table 9) and the relations

$$\Delta G_f^\circ (\text{clinocllore}) = \Delta G^\circ (\text{reaction}) + \Sigma \Delta G_f^\circ (\text{reactants}) \quad (8a)$$

$$\Delta S_f^\circ (\text{clinocllore}) = \Delta S^\circ (\text{reaction}) + \Sigma \Delta S_f^\circ (\text{reactants}). \quad (8b)$$

The "reactants" in Equations 8a and 8b are enstatite, forsterite, spinel, and H_2O (steam). Values of ΔG_f° and ΔS_f° at 1 bar and 298 K for spinel, forsterite, and steam were taken from Robie et al. (1978) (with S° of spinel corrected for 10% Mg and Al disorder according to Navrotsky and Kleppa, 1967), whereas the data for enstatite ($\text{Mg}_2\text{Si}_2\text{O}_6$) were obtained from the calorimetric work of Charlou et al. (1975) and Krupka et al. (1979), yielding

Table 10. Thermochemical data for clinocllore at 1 bar and 298 K

Investigator	ΔG_f° kJ/mol	ΔS_f° J/K·mol	ΔH_f° kJ/mol	S_{298}° J/K·mol
This study	-8220.452 \pm 27	-2186.2 \pm 33	-8871.940 \pm 27	459.4 \pm 33
Helgeson et al. (1978)	-8207.765	-2179.906	-8857.377	465.261
Chernosky (1974)	-8237.88 \pm 33	-2167.3 \pm 12	-8882.63 \pm 37	476.12
Bird and Anderson (1973)	-8260.47 \pm 33	-2188.2 \pm 42*	-8912.56 \pm 36	(457.37 \pm 42)**

* ΔS_f° from Zen (1972)
** Based on ΔS_f° from Zen (1972) and S° for the elements from Robie et al. (1978)

$\Delta H_f^0 = -3097.14 \pm 2.5$ kJ/mol, $\Delta S_f^0 = -585.41 \pm 0.5$ J/(K·mol), and $\Delta G_f^0 = -2922.688 \pm 2.5$ kJ/mol at 1 bar and 298 K. Substituting these data along with the average of the maximum and minimum values of $\Delta G^0 = 169.746 \pm 27$ kJ/mol and $\Delta S^0 = 624.79 \pm 33$ J/(K·mol) for Reaction C into Equations 8a and 8b gives $\Delta G_f^0 = -8220.452 \pm 27$ kJ/mol and $\Delta S_f^0 = -2186.2 \pm 33$ J/(K·mol) for pure clinocllore at 298 K and 1 bar. The extant thermochemical data for clinocllore from various sources are compared in Table 10.

The results of this study are consistent with the compositions and compositional variations of natural chlorite that are observed in ultramafic and calc-silicate assemblages. For example, Frost (1975) found that the most stable chlorite in a contact-metamorphosed serpentinite has the composition $(Mg_{4.8}Al_{1.2})(Si_{2.8}Al_{1.2})O_{10}(OH)_8$ ($X = 1.2$). Rice (1977) found that chlorite in metamorphosed carbonate assemblages also appears to have a composition of $X \cong 1.2$. In addition, Frost (1975) and Pinsent and Hirst (1977) saw distinct increases in the Al content of chlorite with increasing proximity to the thermal contact of contact-metamorphosed peridotites. This increase in the Al content of chlorite with progressive metamorphism agrees with the data in Figures 5 and 6 whereby the composition of chlorite in equilibrium with forsterite and either talc, anthophyllite, or orthopyroxene gradually increases from $X = 1.0$ to $X = 1.2$ with increasing temperature.

As with any experimental study dealing with a simple chemical system, caution must be exercised in extrapolating the results of this study to natural systems that are not appropriate, namely, those with significant amounts of other components (notably Fe), those saturated in silica, or those known to have equilibrated in H_2O -poor environments.

ACKNOWLEDGMENTS

David M. Jenkins gratefully acknowledges the financial support for the work done in partial fulfillment of his doctoral dissertation at the University of Chicago, funded by the National Science Foundation (NSF) grants EAR 78-15939 and 81-07110 to Robert C. Newton, and for the financial support received as a postdoctoral research associate from NSF grant EAR 83-05904 to Julian R. Goldsmith. Joseph V. Chernosky gratefully acknowledges the financial support from the University of Maine Faculty Research Funds and from NSF grants GA-43776 and EAR 79-04092. The manuscript was greatly improved by the constructive reviews of Helen M. Lang, B. Ron Frost, and Jack M. Rice. Thanks are also given to Susan M. Swapp and Charles Geiger for helpful discussions.

Special thanks are given to Cassandra C. Spooner for typing the manuscript. Financial support from NSF grant EAR-8507752 to the first author (DMJ) for manuscript preparation is gratefully acknowledged.

REFERENCES

- Appleman, D. E., and Evans, H. T., Jr. (1973) Job 9214: Indexing and least-squares refinement of powder diffraction data. U.S. National Technical Information Service, PB2-16188.
- Bailey, S.W., and Brown, B.E. (1962) Chlorite polytypism. I. Regular and semirandom one-layer structures. *American Mineralogist*, 47, 819-850.
- Bird, G.W., and Anderson, G.M. (1973) The free energy of formation of magnesian cordierite and phlogopite. *American Journal of Science*, 273, 84-91.
- Bird, G.W., and Fawcett, J.J. (1973) Stability relations of Mg-chlorite-muscovite and quartz between 5 and 10 kbar water pressure. *Journal of Petrology*, 14, 415-428.
- Bradley, W.F. (1959) Current progress in silicate structures. In A. Swineford, Ed. *Proceedings of the Sixth National Conference on Clays and Clay Minerals*, 18-25. Pergamon, New York.
- Burnham, C.W. (1962) Lattice constant refinement. *Carnegie Institution of Washington Year Book* 61, 132-135.
- Burnham, C.W., Hollaway, J.R., and Davis, N.F. (1969) The thermodynamic properties of water to 1000°C and 10,000 bars. *Geological Society of America Special Paper* 132.
- Carroll, D. (1970) Clay minerals: A guide to their identification. *Geological Society of America Special Paper* 126, 1-80.
- Caruso, L.J., and Chernosky, J.V., Jr. (1979) The stability of lizardite. *Canadian Mineralogist*, 17, 757-769.
- Charlu, T.V., Newton, R.C., and Kleppa, O.J. (1975) Enthalpies of formation at 970 K of compounds in the system $MgO-Al_2O_3-SiO_2$ from high temperature solution calorimetry. *Geochimica et Cosmochimica Acta*, 39, 1487-1497.
- Chernosky, J.V., Jr. (1974) The upper stability of clinocllore at low pressure and the free energy of formation of Mg-cordierite. *American Mineralogist*, 59, 496-507.
- (1982) The stability of clinochrysotile. *Canadian Mineralogist*, 20, 19-27.
- Cho, M., and Fawcett, J.J. (1986) A kinetic study of clinocllore and its high temperature equivalent forsterite-cordierite-spinel at 2 kbar water pressure. *American Mineralogist*, 71, 68-77.
- Delany, J.M., and Helgeson, H.C. (1978) Calculation of the thermodynamic consequences of dehydration in subducting oceanic crust to 100 kb and >800°C. *American Journal of Science*, 278, 638-686.
- Fawcett, J.J., and Yoder, H.S., Jr. (1966) Phase relations of chlorites in the system $MgO-Al_2O_3-SiO_2-H_2O$ at 2 kbar water pressure. *American Mineralogist*, 51, 353-380.
- Fleming, P.D., and Fawcett, J.J. (1976) Upper stability of chlorite + quartz in the system $MgO-FeO-Al_2O_3-SiO_2-H_2O$ at 2 kbar water pressure. *American Mineralogist*, 61, 1175-1193.
- Frazer, J.R. (1968) *Applied linear programming*. Prentice-Hall, Englewood Cliffs, New Jersey.
- Frost, B.R. (1975) Contact metamorphism of serpentinite, chlorite blackwall, and rodingite at Paddy-Go-Easy Pass, central Cascades, Washington. *Journal of Petrology*, 16, 272-313.
- Ganguly, J., and Ghose, S. (1979) Aluminous orthopyroxene: Order-disorder, thermodynamic properties, and petrologic implications. *Contributions to Mineralogy and Petrology*, 69, 375-385.
- Gasparik, T., and Newton, R.C. (1984) The reversed alumina contents of orthopyroxene in equilibrium with spinel and forsterite in the system $MgO-Al_2O_3-SiO_2$. *Contributions to Mineralogy and Petrology*, 85, 186-196.
- Gillery, F.H. (1959) The X-ray study of synthetic Mg-Al serpentines and chlorites. *American Mineralogist*, 44, 143-152.
- Gordon, T.M. (1973) Determination of internally consistent thermodynamic data from phase equilibrium experiments. *Journal of Geology*, 81, 199-208.
- Helgeson, H.C., Delany, J.M., Nesbitt, H.W., and Bird, D.K. (1978) Summary and critique of the thermodynamic properties of rock-forming minerals. *American Journal of Science*, 278-A.
- Holland, T.J.B. (1981) Thermodynamic analysis of simple mineral systems. In R.C. Newton et al., Eds. *Thermodynamics of minerals and melts*, 19-34. Springer-Verlag, New York.
- Jenkins, D.M. (1980) Crystallochemical characterization of synthetic Mg-chlorites. *Geological Society of America Abstracts with Programs*, 12, 455.
- (1981) Experimental phase relations of hydrous perido-

- tites modelled in the system H_2O -CaO-MgO-Al₂O₃-SiO₂. Contributions to Mineralogy and Petrology, 77, 166-176.
- (1983) Stability and composition relations of calcic amphiboles in ultramafic rocks. Contributions to Mineralogy and Petrology, 83, 375-384.
- Krupka, K.M., Kerrick, D.M., and Robie, R.A. (1979) Heat capacities of synthetic orthoenstatite and natural anthophyllite from 5 to 1000 K. (abs.) EOS (American Geophysical Union Transactions), 60, 405.
- Lonker, S.W. (1981) The *P-T-X* relations of the cordierite-garnet-sillimanite-quartz equilibrium. American Journal of Science, 281, 1056-1090.
- Martignole, J., and Sisi, J.-C. (1981) Cordierite-garnet-H₂O equilibrium: A geological thermometer, barometer and water fugacity indicator. Contributions to Mineralogy and Petrology, 77, 38-46.
- McOnie, A.W., Fawcett, J.J., and James, R.S. (1975) The stability of intermediate chlorites of the clinocllore-daphnite series at 2 kbar *P*(H₂O). American Mineralogist, 60, 1047-1062.
- Medenbach, O., Maresch, W.V., Mirwald, P.W., and Schreyer, W. (1980) Variation of refractive index of synthetic Mg-cordierite with H₂O content. American Mineralogist, 65, 367-373.
- Mirwald, P.W., and Schreyer, W. (1977) Die stabile und metastabile Abbaureaktion von Mg-cordierit in Talk, Disthen und Quarz und ihre Abhängigkeit vom Gleichgewichtswassergehalt des Cordierits. Fortschritte der Mineralogie, 55, 95-97.
- Navrotsky, A., and Kleppa, O.J. (1967) The thermodynamics of cation distributions in simple spinels. Journal of Inorganic and Nuclear Chemistry, 29, 2701-2714.
- Nelson, B.W., and Roy, R. (1958) Synthesis of the chlorites and their structural and chemical constitution. American Mineralogist, 43, 707-725.
- Newton, R.C., and Wood, B.J. (1979) Thermodynamics of water in cordierite and some petrologic consequences of cordierite as a hydrous phase. Contributions to Mineralogy and Petrology, 68, 391-405.
- Pinsent, R.H., and Hirst, D.M. (1977) The metamorphism of the Blue River ultramafic body, Cassiar, British Columbia, Canada. Journal of Petrology, 18, 567-594.
- Rice, J.M. (1977) Contact metamorphism of impure dolomitic limestone in the Boulder aureole, Montana. Contributions to Mineralogy and Petrology, 59, 237-259.
- Robie, R.A., Bethke, P.M., and Beardsley, K.M. (1967) Selected X-ray crystallographic data, molar volumes and densities of minerals and related substances. U.S. Geological Survey Bulletin 1248.
- Robie, R.A., Hemingway, B.S., and Fisher, J.R. (1978) Thermodynamic properties of minerals and related substances at 298.15 K and 1 bar (10⁵ pascals) pressure and at higher temperatures. U.S. Geological Survey Bulletin 1452.
- Roy, D.M., and Roy, R. (1955) Synthesis and stability of minerals in the system MgO-Al₂O₃-SiO₂-H₂O. American Mineralogist, 40, 147-178.
- Schreyer, W., and Schairer, J.F. (1961) Compositions and structural states of anhydrous Mg-cordierites: A re-investigation of the central part of the system MgO-Al₂O₃-SiO₂. Journal of Petrology, 2, 324-406.
- Schwab, R.G., and Küstner, R.G. (1977) Präzisionsgitterkonstantenbestimmung zur Festlegung röntgenographischer Bestimmungskurven für synthetische Olivine der Mischkristallreihe Forsterit-Fayalit. Neues Jahrbuch für Mineralogie, Monatshefte, 5, 205-215.
- Seifert, F. (1974) Stability of sapphirine: A study of the aluminous part of the system MgO-Al₂O₃-SiO₂-H₂O. Journal of Geology, 82, 173-204.
- Shirozu, H. (1978) Chlorite minerals. In T. Sudo and S. Shimoda, Eds. Clays and clay minerals in Japan. Developments in sedimentology, 26, 243-264. Elsevier-Kodansha, Tokyo.
- Shirozu, H., and Ishida, K. (1982) Infrared study of some 7 Å and 14 Å layer silicates by deuteration. Mineralogical Journal, 11, 161-171.
- Shirozu, H., and Momoi, H. (1972) Synthetic Mg-chlorite in relation to natural chlorite. Mineralogical Journal, 6, 464-476.
- Staudigel, H., and Schreyer, W. (1977) The upper thermal stability of clinocllore, Mg₅Al[Si₃Al₁₀](OH)₈, at 10-35 kbar *P*(H₂O). Contributions to Mineralogy and Petrology, 61, 187-198.
- Velde, B. (1973) Phase equilibria in the system MgO-Al₂O₃-SiO₂-H₂O: Chlorites and associated minerals. Mineralogical Magazine, 39, 297-312.
- Wood, B.J., and Banno, S. (1973) Garnet-orthopyroxene and orthopyroxene-clinopyroxene relationships in simple and complex systems. Contributions to Mineralogy and Petrology, 42, 109-124.
- Yoder, H.S., Jr. (1952) The MgO-Al₂O₃-SiO₂-H₂O system and the related metamorphic facies. American Journal of Science, Bowen Volume, 569-627.
- Zen, E-an. (1960) Metamorphism of lower Paleozoic rocks in the vicinity of the Taconic Range in west-central Vermont. American Mineralogist, 45, 129-175.
- (1972) Gibbs free energy, enthalpy, and entropy of ten rock-forming minerals: Calculations, discrepancies, implications. American Mineralogist, 57, 524-553.

MANUSCRIPT RECEIVED FEBRUARY 7, 1984

MANUSCRIPT ACCEPTED MARCH 18, 1986